Biophysical Journal Volume 74 April 1998 2069–2075

Energy Transfers in the B808–866 Antenna from the Green Bacterium *Chloroflexus aurantiacus*

Vladimir I. Novoderezhkin,* Alexandra S. Taisova,* Zoya G. Fetisova,* Robert E. Blankenship,[#]
Sergei Savikhin,[§] Daniel R. Buck,[§] and Walter S. Struve[§]

*A. N. Belozersky Institute of Physico-Chemical Biology, Moscow State University, Moscow 119899, Russia; [#]the Department of Chemistry and Biochemistry and Center for Early Events in Photosynthesis, Arizona State University, Tempe, Arizona 85287 USA; and [§]Ames Laboratory-USDOE and Department of Chemistry, Iowa State University, Ames, Iowa 50011 USA

ABSTRACT Energy transfers within the B808–866 BChl *a* antenna in chlorosome-membrane complexes from the green photosynthetic bacterium *Chloroflexus aurantiacus* were studied in two-color pump-probe experiments at room temperature. The steady-state spectroscopy and protein sequence of the B808–866 complex are reminiscent of well-studied LH2 antennas from purple bacteria. B808→B866 energy transfers occur with ~2 ps kinetics; this is slower by a factor of ~2 than B800→B850 energy transfers in LH2 complexes from *Rhodopseudomonas acidophila* or *Rhodobacter sphaeroides*. Anisotropy studies show no evidence for intra-B808 energy transfers before the B808→B866 step; intra-B866 processes are reflected in 350–550 fs anisotropy decays. Two-color anisotropies under 808 nm excitation suggest the presence of a B808→B866 channel arising either from direct laser excitation of upper B866 exciton components that overlap the B808 absorption band or from excitation of B866 vibronic bands in nontotally symmetric modes.

INTRODUCTION

Recent reports of three-dimensional structures for the LH2 BChl *a* antennas from the purple photosynthetic bacteria *Rhodopseudomonas acidophila* (McDermott et al., 1995) and *Rhodospirillum molischianum* (Koepke et al., 1996) have stimulated much renewed interest in their electronic structure (Novoderezhkin and Razjivin, 1995; 1996; Sauer et al., 1996; Hu et al., 1997) and energy transfers (Pullerits and Sundström, 1996; Sundström and van Grondelle, 1995). These antennas are $\alpha_N\beta_N$ aggregates with an N-fold proper rotation axis containing N α- and N β-apoproteins in concentric inner and outer rings, respectively. (N varies with the bacterial species and equals 8 and 9 respectively in the LH2 complexes from *Rs. molischianum* and *Rps. acidophila.*) The $3N$ BChl *a* pigments occupy an annular space between the protein helices. N monomeric BChl *a* pigments (responsible for the bulk of the characteristic 800 nm Q_y absorption band) lie flat in the membrane plane interleaved between the β-apoprotein helices. The remaining $2N$ BChl *a* pigments (which are responsible for the intense Q_y absorption band near 850 nm) form a strongly coupled circular aggregate on the periplasmic side of the complex. The alternating resonance interactions between neighboring B850 BChls in *Rps. acidophila* have been variously estimated as 110 and 230 cm^{-1} (Jiminez et al., 1996), 320 and 450 cm^{-1} (Pullerits and Sundström, 1996), and 544 and 754 cm^{-1} (Dracheva et al., 1996). Hu et al. (1997) modeled the B850 absorption spectrum of LH2 from *Rs. molischianum* using 377 and 806 cm^{-1} interactions. The centers of the B800 and B850 rings are mutually displaced along the C_N axis so that the Mg-Mg separations between nearest B800 and B850 pigments are ~18 Å in *Rps. acidophila* (McDermott et al., 1995). The B800 and B850 pigments are connected by carotenoids that may play a major role in downhill energy transfers between them. B800→B850 energy transfers in LH2 complexes from the purple bacterium *Rhodobacter sphaeroides* occur with ~1.8 ps kinetics at 77 K and ~0.7 ps at room temperature (Hess et al., 1995). Similar B800→B850 energy transfer rates have been observed in *Rps. acidophila* (Wu et al., 1996).

Fragmentary evidence suggests that the building blocks of the B808–866 BChl *a* antenna in the green thermophilic bacterium *Chloroflexus aurantiacus* are structurally similar to LH2 complexes from purple bacteria. These pigment-protein complexes surround the P870 reaction centers in the cytoplasmic membrane; in this respect, they resemble LH1 complexes in purple bacteria. Electronic excitations in the oligomeric, light-harvesting 740-nm BChl *c* antenna travel to a 795 nm BChl *a* chlorosome baseplate antenna with multiexponential kinetics (Savikhin et al., 1994; Savikhin et al., 1996) dominated by a 10–40 ps component, the lifetime of which appears to depend on the antenna size (Fetisova et al., 1996). The subsequent ~40-ps BChl *a* 795 excitation decay at room temperature is reportedly mirrored by similar rise kinetics in B808–866 emission (Causgrove et al., 1990; Müller et al., 1990; 1993). Whereas the B808→866 energy transfer time has not previously been measured in the membrane, Vasmel et al. (1986) inferred it to be ~6 ps in a steady-state emission study. Griebenow et al. (1991) observed ~5 ps B808→866 kinetics in isolated complexes using time-correlated photon counting. These energy transfer times are of the same order as (but several times slower than) the B800→B850 kinetics observed in LH2 of purple bacteria (Sundström and van Grondelle, 1995; Pullerits and Sundström, 1996). Excitation trapping from the B808–866

Received for publication 31 July 1997 and in final form 6 January 1998.

Address reprint requests to Dr. Walter S. Struve, Department of Chemistry, Iowa State University, Gilman Hall, Ames, IA 50011-3111. Tel.: 515-294-4276; Fax: 515-294-1699; E-mail: wstruve@ameslab.gov.

0006-3495/98/04/2069/07 $2.00

antenna to oxidized ($P870^+$) reaction centers requires ~200 ps (Nuijs et al., 1986; Mimuro et al., 1989; Müller et al., 1993). Excitation trapping at reduced reaction centers has been observed with 43-ps kinetics by Causgrove et al. (1990) and with 90-ps kinetics by Müller et al. (1993).

The B808–866 and LH2 antennas exhibit parallels in their protein structure (Wechsler et al., 1985; 1987; Zuber and Brunisholz, 1991) as well as in their absorption spectra and energy transfer kinetics. The B808–866 complex contains α- and β-polypeptides in 1:1 ratio. The α- and β-proteins (containing 44 and 51 residues, respectively) both show 3-domain structures reminiscent of LH2; they exhibit 27–30% sequence homologies to the α- and β-polypeptides of LH2. Each B808–866 polypeptide has, within its hydrophobic α-helical domain, a histidine residue that can coordinate a BChl pigment.

We investigate here the excited state kinetics of membrane-bound B808–866 complexes from *C. aurantiacus* under femtosecond resolution. This study enables a direct comparison with the more extensively studied LH2 complexes from *Rps. acidophila* and *Rb. sphaeroides* and lends additional insight into LH2 work previously reported by one of our groups (Wu et al., 1996; Savikhin and Struve, 1996). The present study focuses on the phenomenological B808–866 kinetics. Many groups have been concerned with exciton structure and localization in LH2 (Alden et al; 1997; Chachisvilis et al.; 1997; Meier et al., 1997; Monshouwer et al., 1997; Pullerits et al., 1996). A theoretical study of our results based on exciton models will be deferred to a later article (V. Novoderezhkin, A. Taisova, and Z. Fetisova, work in progress).

MATERIALS AND METHODS

Cells of *C. aurantiacus* were grown photoheterotrophically as described by Pierson and Castenholz (1992). The chlorosome-membrane complexes were prepared according to Feick and Fuller (1984).

The self-mode-locked Ti:sapphire laser and pump-probe optics have been described elsewhere (Savikhin and Struve, 1994; Savikhin et al., 1994). In one-color experiments, the laser output was tuned with a single-plate birefringent filter producing an ~80-fs pulse width and an ~10-nm spectral bandwidth. In two-color experiments, the birefringent filter was omitted yielding ~40-fs pulses and ~20- to 40-nm bandwidth. The pump and probe spectra were independently shaped using ~7-nm bandpass interference filters (CVI Corp., Albuquerque, NM); wavelength fine tuning was achieved by tilting the filters. The laser cross-correlation in two-color experiments was typically 250–300 fs. The radio frequency multiple modulation detector and electronics were superseded by a new design in which the probe beam-detecting photodiode was incorporated into a regulatory light chain loop tuned to the radio detection frequency (Savikhin, 1995). Chlorosome membrane complex (CMC) samples from *C. aurantiacus* were housed in a high-speed centrifugal sample cell (Savikhin et al., 1993) that provided 4 m/s sample travel through the laser beams. This arrangement yielded a sample turnover time of ~6 μs. Excitation pulses generally excited one BChl *a* pigment out of 6000–30,000 (average pump power <0.5 mW at ~75 MHz repetition rate); annihilation effects were absent because ΔA profiles showed no variation with laser power. CMC sample optical densities were typically 0.3–0.4 at 808 nm. The apparatus instrument function used in deconvolutions was recorded concurrently with every pump-probe scan by focusing parts of the pump and probe beams into a $LiIO_3$ nonlinear crystal. The laser pump and probe spectra were measured during experiments using a Czerny-Turner monochromator (7.9 nm/mm dispersion) with its output imaged onto the linear CCD array of a Unidata BP2048 beam profiler.

CMC absorption difference spectra were compiled by amassing two-color pump-probe profiles for a number (up to 18) of probe wavelengths under fixed pump wavelength. Whereas changes in probe wavelength entailed minor reoptimization in probe beam alignment, the precision in relative amplitudes of the resulting pump-probe profiles was not worse than 5%.

RESULTS

B808→B866 energy transfer

CMCs from *C. aurantiacus* grown under high light conditions ($A_{740}/A_{800} \sim 8$) were excited at 808 nm at room temperature and probed at 18 wavelengths from 801 to 901 nm. The CMC steady-state absorption spectrum remained essentially unchanged in the B808–866 region during the course of the experiments. The resulting two-color isotropic absorption difference profiles are shown in Fig. 1. This Figure accurately reflects the relative signal amplitudes for different probe wavelengths; the 808-nm excitation laser conditions were identical for all profiles, and the probe pulse intensities were separately measured with a monitor photodiode for mutual normalization at different probe wavelengths. At probe wavelengths from 801 to 820 nm, an initial photobleaching/stimulated emission (PB/SE) signal decays with primarily ~2 ps kinetics to a (sometimes very small) residual excited state absorption (ESA) signal. At probe wavelengths from 831 to 861 nm, the initial signal is dominated by a ~2 ps ESA rise component; at longer probe wavelengths out to 901 nm, the principal initial feature is a PB/SE rise component with a time constant of 1.5–1.9 ps. Another perspective is given in Fig. 2, which shows absorption difference spectra at fixed time delays (150 fs and 10 ps) assembled from the profiles in Fig. 1. These ΔA spectra are superimposed on the CMC steady-state absorption spectrum measured in the same rotating absorption cell used in pump-probe experiments. At 150 fs, which overlaps the laser cross-correlation function of typically 250–300 fs, the signal exhibits a B808 PB/SE maximum at 810–815 nm combined with a nascent B866 PB/SE maximum near 880 nm. By 10 ps, which is several times longer than the ~2-ps component observed in early time evolution of the profiles in Fig. 1, the B808 PB/SE spectrum has disappeared, and the B866 absorption difference spectrum is well developed. The latter spectrum shows an intense 880-nm PB/SE peak accompanied by a pronounced ESA maximum at ~850 nm. (This ESA feature is already noticeable at 150 fs.) This sigmoid ΔA spectrum with a major ESA peak to the blue of the PB/SE peak is characteristic of strongly coupled circular aggregates with transition moments essentially tangential to the periphery and in the plane of the circle (Sauer et. al, 1996; Hu et al., 1997) — regardless of whether the excitons are fully delocalized, or localized to a subset of the BChl pigments in the ring (Pullerits and Sundström, 1996). The 1.5- to 2-ps lifetime components are reasonably ascribed to a B808→B866 energy transfer step. For comparison, the B800→B850 energy transfer occurs with 0.7-ps kinetics in LH2 complexes from *Rb. sphaeroides* at room temperature (Hess et al., 1995).

The PB/SE rise behavior in the two-color profiles for probe wavelengths near the B866 absorption band, which is

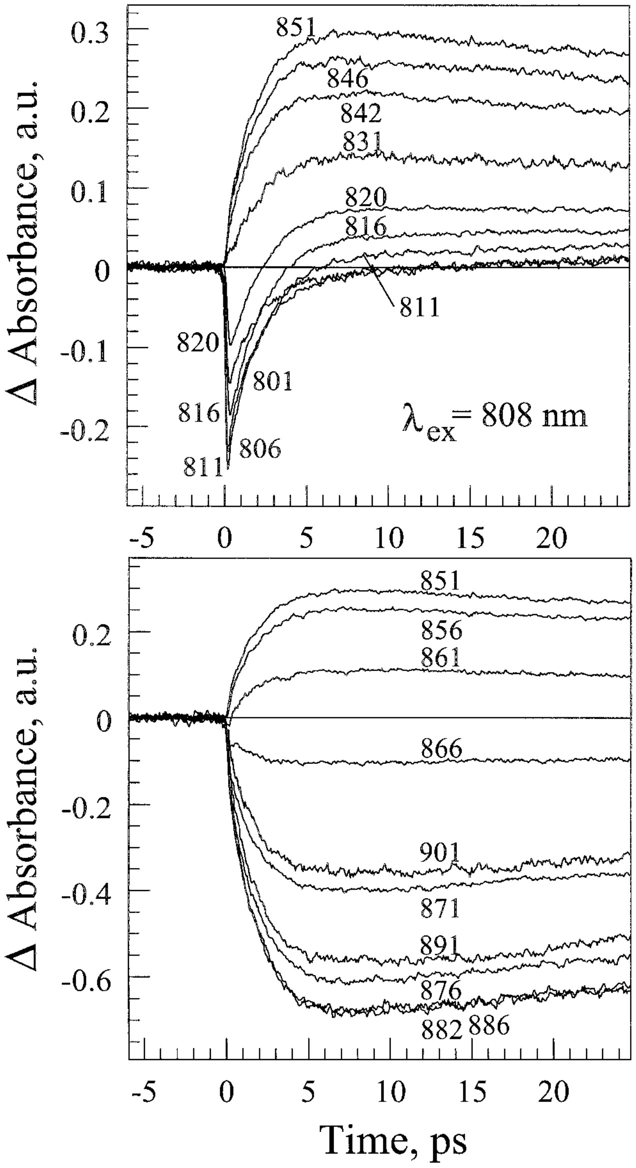

FIGURE 1 Isotropic two-color profiles for CMCs from *C. aurantiacus* excited at 808 nm at room temperature and probed at several wavelengths from 801 to 901 nm. Signals for different probe wavelengths are mutually normalized; absorbance units are otherwise arbitrary. Positive and negative signals correspond to ESA and PB/SE, respectively.

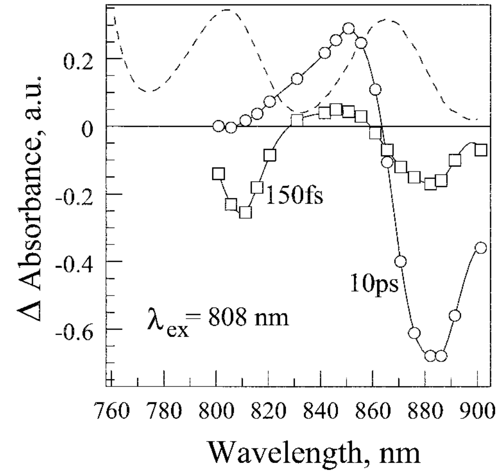

FIGURE 2 Absorption difference spectra of CMCs at fixed time delays, 150 fs (□) and 10 ps (○) after 808-nm excitation, evaluated from the isotropic profiles in Fig. 1. CMC steady-state absorption spectrum is superimposed (*dashed curve*), showing BChl *a* band maxima at 808 and 866 nm.

dominated by a component with lifetime 1.5–1.9 ps (cf. Fig. 1), also shows a prompt PB/SE component even though the 808-nm pump wavelengths do not overlap the B866 spectrum. This prompt component contains some 20% of the total PB/SE rise amplitude (Table 1). In principle, the prompt amplitude could arise from the red tail of the B808 SE spectrum, as was suggested earlier for LH2 from *Rb. sphaeroides* (Savikhin and Struve, 1996). However, anisotropy measurements suggest that the prompt component stems instead from direct excitation of a B866 vibronic or weakly allowed upper exciton component that overlaps the B808 spectrum (see below). A long PB/SE or ESA decay component, with a lifetime of typically 150–200 ps (Table 1), describes the asymptotic behavior in all of the two-color profiles in Fig. 1. This lifetime is not accurately determined in the maximum time windows used here (24 ps), but it is commensurate with reported B808–866 excitation trapping times in the presence of oxidized reaction centers (Nuijs et al., 1986; Mimuro et al., 1989; Müller et al., 1993).

Two-color anisotropies were obtained by exciting CMCs at 808 nm and probing at several wavelengths from 851 to 901 nm (Table 2). These wavelengths span across both the ESA and PB/SE segments of the asymptotic B866 Δ*A* spectrum (Fig. 2). Single-exponential fits of *r(t)* in the time

TABLE 1 Optimized Parameters from Multiexponential Fits to Two-Color Isotropic Absorption Difference Profiles for *C. aurantiacus* CMCs Excited at 808 nm

Probe λ, nm	τ_1 (A_1)	τ_2 (A_2)	τ_3 (A_3)	τ_4 (A_4)*	χ^2
811		2.4 (1072)		>80 (100)	
820		2.5 (−250)		>80 (100)	
831	<0.1 (2)	2.2 (−102)		>80 (100)	29
	<0.1 (−14)	1.7 (−101)	0.9 (42)	>80 (58)	17
842	<0.1 (−14)	1.8 (−86)		>80 (100)	
851	<0.1 (−19)	1.7 (−81)		>80 (100)	13
	<0.1 (−19)	2.0 (−81)	8 (2)	>80 (98)	8
861	0.18 (−44)	1.9 (−100)		>80 (100)	
866	0.12 (−42)	1.3 (38)		>80 (−100)	
871	<0.2 (24)	1.9 (76)		>80 (−100)	
882	<0.2 (20)	1.9 (80)		>80 (−100)	
891	<0.2 (20)	1.9 (80)		>80 (−100)	55
	<0.2 (12)	1.5 (64)	9 (22)	>80 (−100)	43
901	<0.2 (19)	1.8 (81)		>80 (−100)	54
	<0.2 (13)	1.5 (67)	8 (20)	>80 (−100)	51

All lifetimes are in ps. Positive amplitudes correspond to ESA decay and/or PB/SE rise; amplitudes in most cases are normalized so that absolute value of long component amplitude is 100. Fitting window is 24 ps. χ^2 values (listed for contrasting fits to same profile) are in arbitrary units.

*The lifetime τ_4 varied from 88–208 ps, several times larger than the time window.

TABLE 2 Parameters from Single-Exponential Fits to Two-Color Anisotropy Decays for *C. aurantiacus* CMCs Excited at 808 nm

Probe λ, nm	r (0)	τ (A)	r (∞)
851		0.9 (0.09)	−0.05
861		0.7 (0.11)	−0.09
871	0.24	0.8 (0.10)	−0.05
882	0.12	0.9 (0.09)	−0.02
901	0.12	1.1 (0.10)	−0.04

All lifetimes are in ps; fitting window is 8 ps.

window of 200 fs to 8 ps yield lifetimes of 0.7–1.1 ps and nominal initial anisotropies $r(0)$ considerably less than 0.4 (Table 2). Part of the reason for these $r(0)$ values is illustrated by the polarized absorption difference profiles for the 808→871-nm experiment, as shown in Fig. 3. In this case, a rapid initial drop in $r(t)$, which is not accounted for in the single-exponential fits in Table 2, stems from a rapid (≤200 fs) decay in $|\Delta A_{\|}(t)|$, which is not paralleled by a similar decay in $|\Delta A_{\perp}(t)|$. The anisotropies then decay with 0.7–1.1 ps kinetics to $r(\infty) = -0.02$ to -0.09 (Table 2). The origin of the fast anisotropy decay component is unclear. It may arise because some 20% of the CMCs are excited into a weakly allowed B866 exciton component that overlaps the B808 band, or it may originate from excitation of CMCs into B866 levels with vibrational energy in nontotally symmetric modes. (Vibrational relaxation of levels excited in totally symmetric modes would not cause anisotropy decay. To our knowledge, the extent of vibronic coupling in the BChl *a* Q_y absorption spectrum is unknown.) The fast anisotropy kinetics would then correspond either to interexciton state relaxation or vibrational cooling within the B866 manifold. The negative final anisotropy (−0.09) observed at 861 nm is unsurprising because excited absorption dominates the signal at that wavelength at long times (cf. the 10-ps absorption difference spectrum in Fig. 2). For 882 nm, which is close to the asymptotic B866 PB/SE maximum, $r(\infty)$ is close to zero.

B866↔B866 energy transfer

CMCs from chlorosomes grown under high light conditions were subjected to two-color experiments at room temperature analogous to the ones in Fig. 1, except that the pump wavelength was centered at 882 nm (at the red edge of the B866-nm band) instead of at 808 nm. The resulting isotropic profiles are shown in Fig. 4. In all cases, the major decay component exhibits a lifetime considerably greater than the 8-ps window. Minor components appear with lifetimes in the hundreds of femtoseconds and ~2 ps (Table 3). Some spectral evolution nominally occurs, as shown by the absorption difference spectra assembled in Fig. 5 for the time delays, 40 fs and 1 ps. The zero-crossing point between the ESA region migrates several nanometers to the blue in this interval; the absorption difference signal in the 882→866-nm experiment correspondingly switches from ESA to PB/SE within 300 fs (Fig. 4). Although it is tempting to assign these subpicosecond events to intra-B866 energy transfers, Chachisvilis and Sundström (1996) have shown that similar profiles can arise from tunneling contributions to optical coherences in the region of pulse overlap in pseudo-two-color pump-probe experiments when the probe wavelength lies near the zero-crossing point (as is the case in this 882→866-nm profile). The 1-ps absorption difference spectrum coincides (within 5% error) with the 10-ps absorption difference spectrum for CMCs excited at 808 nm (cf. Fig. 2).

An 882-nm one-color anisotropy decay (not shown) nominally initializes at $r(0) = 0.34$. However, this value is

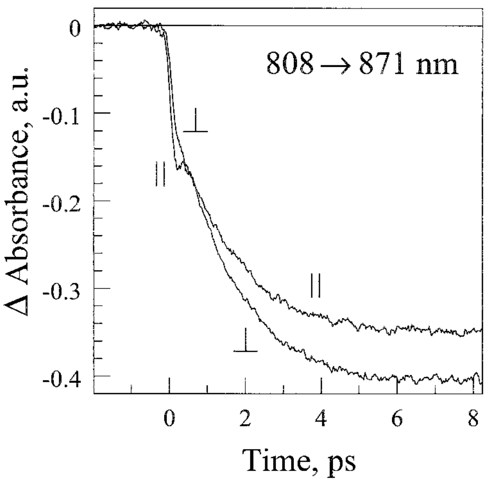

FIGURE 3 Polarized absorption difference profiles $\Delta A_{\|}(t)$, $\Delta A_{\perp}(t)$ for CMCs in 808→871-nm two-color experiment. Signals are dominated by PB/SE throughout. Aside from "prompt" decay component (see text), a single-exponential fit to $r(t)$ for t between 200 fs and 8 ps yields an 800-fs anisotropy decay time.

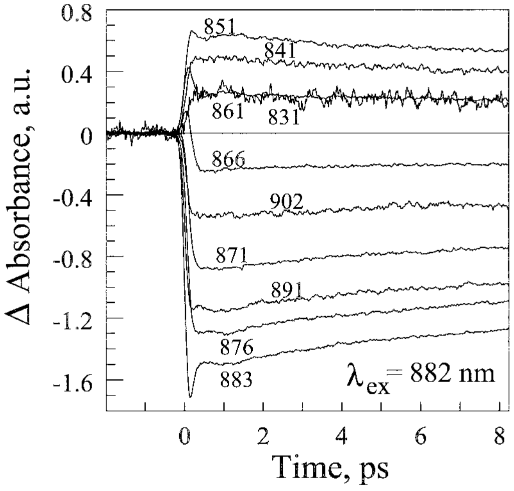

FIGURE 4 Isotropic two-color profiles for CMCs from *C. aurantiacus* excited at 882 nm at room temperature and probed at several wavelengths from 831 to 902 nm. Signals for different probe wavelengths are mutually normalized; absorbance units are otherwise arbitrary. Positive and negative signals correspond to ESA and PB/SE, respectively.

TABLE 3 Parameters from Multiexponential Fits to Selected Two-Color Isotropic Profiles for CMCs Excited at 882 nm

Probe λ, nm	τ_1 (A_1)	τ_2 (A_2)	τ_3 (A_3)	τ_4 (A_4)*	χ^2
866	<0.1 (827)		2.2 (−10)	>50 (−90)	
882	<0.1 (−6)		2.4 (−5)	>50 (−95)	76
	<0.1 (−7)	0.75 (13)	1.7 (−17)	>50 (−83)	34
891	<0.1 (−2)		2.0 (−6)	>50 (−94)	109
	<0.1 (−4)	0.42 (13)	1.5 (−12)	>50 (−88)	80

All lifetimes are in ps. Amplitudes are defined so that the sum of amplitudes for components with a lifetime >1-ps sum to −100.

*The lifetime τ_4 varied from 59–83 ps, several times larger than the 8-ps time window.

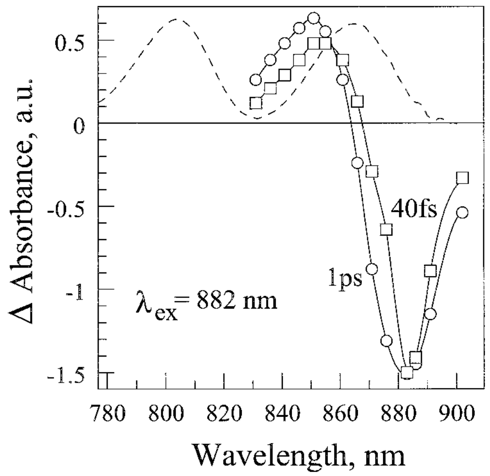

FIGURE 5 Absorption difference spectra of CMCs at fixed time delays, 40 fs (□) and 1 ps (○) after 882-nm excitation, evaluated from the isotropic profiles in Fig. 4. CMC steady-state absorption spectrum is superimposed, showing BChl *a* band maxima at 808 and 866 nm.

certainly influenced by convolution with the laser autocorrelation function (102 fs full width at half maximum) and possibly by a coherent spike. A single exponential fit to this anisotropy function in the time window of 0.15 to 8.0 ps yielded a component with an amplitude of 0.17 and a decay time of 330 fs; the residual anisotropy r(∞) was 0.102. (This decay time is well in excess of the autocorrelation half width at half maximum and thus corresponds to true molecular response.) A biexponential fit in the same window yielded components with the lifetimes (amplitudes) of 150 fs (0.24) and 910 fs (0.04); the residual anisotropy was 0.100. For comparison, the B850 antenna of isolated LH2 complexes from *Rb. sphaeroides* (Pullerits and Sundström, 1996) exhibits an 864-nm one-color anisotropy decay time of 130 fs at room temperature. Single-exponential fits to a series of two-color anisotropies accumulated under 882-nm excitation (probe wavelengths 841, 851, 871, and 882 nm; laser cross-correlation 250–300 fs) yielded lifetimes ranging from 350–550 fs. The final anisotropies varied from ~0.07 (841 and 851 nm) to ~0.10 (871 and 882 nm).

B808↔B808 energy transfer

Fig. 6 shows an 808-nm one-color anisotropy (with the corresponding polarized absorption difference signals) for CMCs from *C. aurantiacus* in 8- and 82-ps time windows. Here *r(t)* remains at ~0.38 for the first picosecond, rises during the next few picoseconds during the B808→B866 energy transfer, becomes negative as the isotropic signal ($\Delta A_{\|} + 2\Delta A_{\perp}$) changes sign, and finally decays toward zero with kinetics in the tens of picoseconds. The anomalous rise behavior in *r*(*t*) stems from growth in B866 ESA that accompanies B808→B866 energy transfer. The ESA signal at 808 nm from emergent B866 is essentially depolarized with the result that the polarized absorption difference signals $\Delta A_{\|}$ and $\Delta A_{\perp}$ (initially dominated by B808 PB/SE) both shift upward in concert. The final, slow anisotropy decay in the tens of picoseconds (at times in which the isotropic absorption difference signal has decayed to <5% of its initial value) may originate from a small fraction of B808 pigments that are kinetically weakly coupled. Alternatively, the 7-nm full width at half maximum 808-nm excitation spectrum may overlap the red edge of the Q_y absorption band of the baseplate B795 antenna, which is believed to transfer excitation to the B808–866 antenna with ~40-ps kinetics (Causgrove et al., 1990; Müller et al., 1990; 1993). As *r*(*t*) at times <1 ps shows no discernible decay, there is little evidence in Fig. 6 for subpicosecond intra-B808 energy transfers.

Intra-B808 isotropic two-color profiles were also obtained for combinations of pump and probe wavelengths between 770 and 820 nm. The 790→820-nm profile shows no PB/SE rise feature slower than ~200 fs, which approaches the laser cross-correlation width. This fact, combined with absence of a femtosecond anisotropy decay component in Fig. 6 suggests that the B808 pigments func-

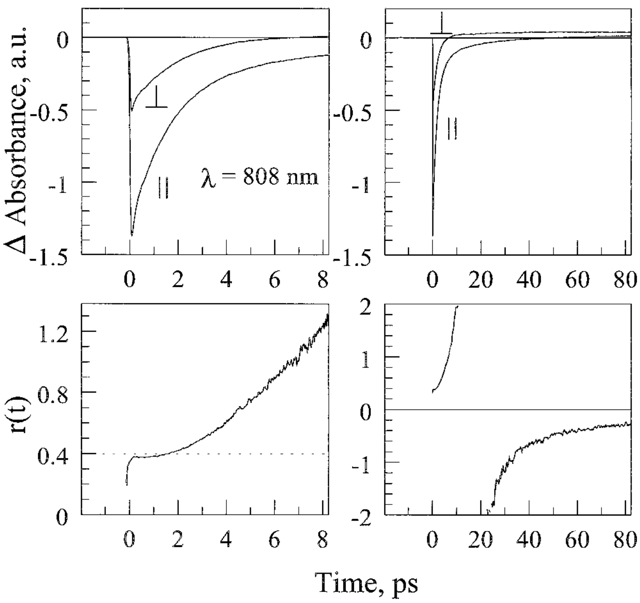

FIGURE 6 Polarized absorption difference signals and anisotropy for CMCs in 808-nm one-color experiment; time windows are 8 ps (*left*) and 82 ps (*right*).

tion essentially as monomeric BChls and that intra-B808 energy transfers are infrequent before B808→B866 energy transfer. The 790→820-nm profile (initially dominated by PB/SE) exhibits PB/SE decay components with lifetimes 2.1 ps (27%) and 41 ps (73%). Analysis of an 800-nm one-color profile yields similar PB/SE decay times but with the amplitudes redistributed in favor of the short-lifetime component: 1.7 ps (57%) and 28 ps (43%). This suggests that the longer component may result from excitation of the B795 BChl *a* baseplate antenna, as shifting the excitation wavelength to the red from the B795 band diminishes the amplitude of this component.

DISCUSSION

The B808→B866 room temperature energy transfer kinetics (as reflected by the 1.5–2 ps components in our two-color experiments, cf. Table 1) bear an order-of-magnitude resemblance to B800–850 energy transfers observed in several purple bacterial species. Hess et al. (1995) reported 700-fs kinetics for this process in *Rb. sphaeroides* at room temperature; the B800→B850 transfers are decelerated to 1.8 ps and 2.4 ps at 77 and 4 K (Hess et al., 1995; Reddy et al., 1992; Van der Laan et al., 1990). The corresponding B800→B850 energy transfer takes ~1.6 and 1.1 ps at 19 and 130 K, respectively, in a strain of *Rps. acidophila* (Wu et al., 1996). Hence, the room temperature kinetics for B808→B866 energy transfers in *C. aurantiacus* CMCs appear to be slower by a factor of ~2 than for the B800→B850 processes in LH2 of purple bacteria. However, they are appreciably faster than the ~5-ps kinetics reported for isolated B808–866 particles (Griebenow et al., 1991). Another kinetic analogy between B808–866 and LH2 appears in the B866 anisotropy decays. A single-exponential fit to an 882-nm one-color anisotropy yields the lifetime 330 fs; similar fits to two-color anisotropies within the B866 band yield lifetimes ranging from 350 to 550 fs. These lifetimes are ~2.5–4 times longer than the 130-fs one-color anisotropy decay found at 864 nm for the LH2 complex of *Rb. sphaeroides* (Pullerits and Sundström, 1996).

We find no clear indications for intra-B808 energy transfers before the 1.5–2 ps B808→B866 step in CMCs from *C. aurantiacus*. No risetimes are found corresponding to downhill energy transfers within B808 in two-color experiments, and the 808-nm one-color anisotropy (Fig. 6) does not decay appreciably from $r(0)$ ~0.38 during the B808 antenna lifetime. This contrasts with the well-established femtosecond B800 intraband kinetics in LH2. Wu et al. (1996) observed B800 spectral evolution in LH2 from *Rps. acidophila* in which an initial ~800-nm PB/SE peak redshifts with ~400-fs kinetics to ~805 nm at 19 K. Hess et al. (1995) reported B800 intraband transfer times increasing from 300 to 600 fs in one-color experiments when the laser wavelength was tuned across the band from the blue to red; similar behavior was noted by Monshouwer et al. (1995). Possible mechanisms for such rapid B800 intraband kinetics in LH2, which are of considerable interest because the dipole-dipole interactions between B800 pigments are expected to be small compared with the static disorder, have recently been discussed by Kühn and Sundström (1997).

We similarly find little evidence for spectral equilibration within B866 beyond early-time effects attributable to optical coherences in the region of laser pulse overlap. For example, the only PB/SE rise feature that emerges from an 850→875-nm two-color experiment on B866 is a 530-fs component with 3% amplitude; 97% of the rise behavior in this profile is prompt. In contrast, downhill two-color experiments within the B850 spectrum of an LH1-free mutant of *Rb. sphaeroides* (Savikhin and Struve, 1996) yield a wealth of subpicosecond rise features (100–300 fs) that dominate the PB/SE rise kinetics in that antenna. The B866 antenna does exhibit anisotropy decay components that appear to be analogous to the 130-fs component found in B850 of *Rb. sphaeroides*, however; so intra-B866 processes clearly do occur. The kinetic effects of diagonal energy disorder may thus be less marked in B866 than in B850. Additional studies with varied excitation wavelength and lower temperatures would help to clarify this point.

The prompt PB/SE components in the B808→866 two-color experiments combined with the corresponding anisotropies (cf. Fig. 3) are especially intriguing in the context of prior speculation (Wu et al., 1996) that direct excitation at 800 nm of higher-lying B850 exciton levels may provide a channel for rapid population of the levels responsible for the intense B850 absorption band in LH2 from *Rps. acidophila*. Exciton simulations (Sauer et al., 1996; Hu et al., 1997) predict the existence of such levels, but their location cannot be independently assigned because the BChl *a* site energies and interactions are uncertain. Our study indicates that this mechanism may provide a major channel for B808→866 energy transfers in the present antenna. In this scenario, some 20% of the excitation in the lowest allowed B866 levels arises from direct excitation of the upper B866 exciton components, whereas the remainder stems from true B808→B866 energy transfers with ~2-ps kinetics.

The Ames Laboratory is operated for the U. S. Department of Energy by Iowa State University under Contract No. W-7405-Eng-82. This work was supported in part by the Division of Chemical Sciences, Office of Basic Energy Sciences (to WSS) and in part by Grant DE-FG-03–97ER20267 (to REB). This is publication number 345 from the Arizona State University Center for the Study of Early Events in Photosynthesis. This research was made possible in part by Grant 96–04-49205 from the Russian Foundation for Basic Research (to ZGF) and a grant from the Russian Universities Foundation (to ZGF). We thank John Lopez for his technical assistance.

REFERENCES

Alden, R. G., E. Johnson, V. Nagarajan, W. W. Parson, C. J. Law, and R. G. Cogdell. 1997. Calculations of spectroscopic properties of the LH2 bacteriochlorophyll-protein antenna complex from *Rhodopseudomonas acidophila*. *J. Phys. Chem.* B101:4667–4680.

Causgrove, T. P., D. C. Brune, J. Wang, B. P. Wittmershaus, and R. E. Blankenship. 1990. Energy transfer kinetics in whole cells and isolated chlorosomes of green photosynthetic bacteria. *Photosynth. Res.* 26: 39–48.

Chachisvilis, M., O. Kühn, T. Pullerits, and V. Sundström. 1997. Excitons in photosynthetic purple bacteria: wavelike motion or incoherent hopping? *J. Phys. Chem.* B101:7275–7283.

Chachisvilis, M., and V. Sundström. 1996. The tunnelling contributions to optical coherence in femtosecond pump-probe spectroscopy of the three level system. *J. Chem. Phys.* 104:5734–5744.

Dracheva, T. V., V. I. Novoderezhkin, and A. P. Razjivin. 1996. Exciton delocalization in the antenna of purple bacteria: exciton spectra calculations using X-ray data and experimental site inhomogeneity. *FEBS Lett.* 378:81–84.

Feick, R. G., and R. C. Fuller. 1984. Topography of the photosynthetic apparatus of *Chloroflexus aurantiacus*. *Biochemistry.* 23:3693–3700.

Fetisova, Z. G., A. M. Freiberg, K. Mauring, V. I. Novoderezhkin, A. S. Taisova, and K. E. Timpmann. 1996. Excitation energy transfer in chlorosomes of green bacteria: theoretical and experimental studies. *Biophys. J.* 71:995–1010.

Griebenow, K., M. G. Müller, and A. R. Holzwarth. 1991. Pigment organization and energy transfer in green bacteria. 3. Picosecond energy transfer kinetics within the B808–866 bacteriochlorophyll a antenna complex isolated from *Chloroflexus aurantiacus*. *Biochim. Biophys. Acta.* 1059:226–232.

Hess, S., E. Åkesson, R. J. Cogdell, T. Pullerits, and V. Sundström. 1995. Energy transfer in spectrally inhomogeneous light-harvesting pigment-protein complexes of purple bacteria. *Biophys. J.* 69:2211–2225.

Hu, X., T. Ritz, A. Damjanovic, and K. Schulten. 1997. Pigment organization and transfer of electronic excitation in the purple bacteria. *J. Phys. Chem.* 101:3854–3871.

Jiminez, R., S. N. Dikshit, S. E. Bradforth, and G. R. Fleming. 1996. Electronic excitation transfer in the LH2 complex of *Rhodobacter sphaeroides*. *J. Phys. Chem.* 100:6825–6834.

Koepke, J., X. Hu, C. Muenke, K. Schulten, and H. Michel. 1996. The crystal structure of the light-harvesting complex II (B800–850) from *Rhodospirillum molischianum*. *Structure.* 4:581–597.

Kühn, O., and V. Sundström. 1997. Energy transfer and relaxation dynamics in light-harvesting antenna complexes of photosynthetic bacteria. *J. Phys. Chem.* B101:3432–3440.

McDermott, G., S. M. Prince, A. A. Freer, A. M. Hawthornthwaite-Lawless, M. Z. Papiz, R. J. Cogdell, and N. W. Isaacs. 1995. Crystal structure of an integral membrane light-harvesting complex from photosynthetic bacteria. *Nature.* 374:517–521.

Meier, T., V. Chernyak, and S. Mukamel. 1997. Multiple exciton coherence sizes in photosynthetic antenna complexes viewed by pump-probe spectroscopy. *J. Phys. Chem.* B101:7332–7342.

Mimuro, M., T. Nozawa, N. Tamai, K. Shimada, I. Yamazaki, S. Lin, R. S. Knox, B. P. Wittmershaus, D. C. Brune, and R. E. Blankenship. 1989. Excitation energy flow in chlorosome antennas of green photosynthetic bacteria. *J. Phys. Chem.* 93:7503–7509.

Monshouwer, R., M. Abrahamsson, R. van Mourik, and R. van Grondelle. 1997. Superradiance and exciton delocalization in bacterial photosynthetic light-harvesting systems. *J. Phys. Chem.* B101:7241–7248.

Monshouwer, R., I. O. DeZerate, F. van Mourik, and R. van Grondelle. 1995. Low intensity pump-probe spectroscopy on the B800 to B850 transfer in the light harvesting 2 complex of *Rhodobacter sphaeroides*. *Chem. Phys. Lett.* 246:341.

Müller, M. G., K. Griebenow, and A. R. Holzwarth. 1990. Fluorescence lifetime measurements of energy transfer in chlorosomes and living cells of *Chloroflexus aurantiacus* OK 70-fl. *In* Current Research in Photosynthesis, Vol. II. M. Baltsheffsky, editors. Kluwer, Dordrecht. 177–180.

Müller, M. G., K. Griebenow, and A. R. Holzwarth. 1993. Picosecond energy transfer and trapping kinetics in living cells of the green bacterium *Chloroflexus aurantiacus*. *Biochim. Biophys. Acta.* 1144:161–169.

Novoderezhkin, V. I., and A. P. Razjivin. 1995. Exciton dynamics in circular aggregates: application to antenna of photosynthetic purple bacteria. *Biophys. J.* 68:1089–1100.

Novoderezhkin, V. I., and A. P. Razjivin. 1996. The theory of Förster-type migration between clusters of strongly interacting molecules: Application to light-harvesting complexes of purple bacteria. *Chem. Phys.* 211:203–214.

Nuijs, A. M., H. Vasmel, L. N. M. Duysens, and J. Amesz. 1986. Antenna and reaction-center processes upon picosecond-flash excitation of membranes of the green photosynthetic bacterium *Chloroflexus aurantiacus*. *Biochim. Biophys. Acta.* 849:316–324.

Pierson, B. K., and R. W. Castenholz. 1992. The family *Chloroflexaceae*. *In* The Prokaryotes. A. Balows, H. G. Trüper, M. Dworkin, K. H. Schliefer, and W. Harder, editors. Springer-Verlag, Berlin. 3754–3774.

Pullerits, T., M. Chachisvilis, and V. Sundström. 1996. Exciton delocalization length in the B850 antenna of *Rhodobacter sphaeroides*. *J. Phys. Chem.* 100:10787–10792.

Pullerits, T., and V. Sundström. 1996. Photosynthetic light-harvesting pigment-protein complexes: toward understanding how and why. *Acc. Chem. Res.* 29:381–389.

Reddy, N. R. S., R. Picorel, and G. J. Small. 1992. B896 and B870 components of the Rhodobacter sphaeroides antenna: a hole burning study. *J. Phys. Chem.* 96:6458–6464.

Sauer, K., R. J. Cogdell, S. M. Prince, A. Freer, N. W. Isaacs, and H. Scheer. 1996. Structure-based calculations of the optical spectra of the LH2 bacteriochlorophyll-protein complex from *Rhodopseudomonas acidophila*. *Photochem. Photobiol.* 64:564–576.

Savikhin, S. 1995. Shot-noise-limited detection of absorbance changes induced by subpicojoule laser pulses in optical pump-probe experiments. *Rev. Sci. Instrum.* 66:4470–4474.

Savikhin, S., and W. S. Struve, 1994. Ultrafast energy transfer in FMO trimers from the green bacterium *Chlorobium tepidum*. *Biochemistry.* 33:11200–11208.

Savikhin, S., and W. S. Struve. 1996. Temperature dependence of electronic energy transfers within B850 antennae of the NF57 mutant of the purple bacterium *Rhodobacter sphaeroides*. *Chem. Phys.* 210:91–100.

Savikhin, S., T. Wells, P.-S. Song, and W. S. Struve. 1993. Ultrafast pump-probe spectroscopy of native etiolated oat phytochrome. *Biochemistry.* 32:7512–7518.

Savikhin, S., Y. Zhu, R. E. Blankenship, and W. S. Struve. 1996. Ultrafast energy transfer in chlorosomes from the green photosynthetic bacterium *Chloroflexus aurantiacus*. *J. Phys. Chem.* 100:3320–3322.

Savikhin, S., Y. Zhu, S. Lin, R. E. Blankenship, and W. S. Struve. 1994. Femtosecond spectroscopy of chlorosome antennas from the green photosynthetic bacterium *Chloroflexus aurantiacus*. *J. Phys. Chem.* 98: 10322–10334.

Sundström, V., and R. van Grondelle. 1995. Kinetics of excitation transfer and trapping in purple bacteria. *In* Anoxygenic Photosynthetic Bacteria. R. E. Blankenship, M. T. Madigan, and C. E. Bauer, editors. Kluwer, Dordrecht. 349–372.

Van der Laan, R., Th. Schmidt, R. W. Visschers, K. J. Visscher, R. van Grondelle, and S. Völker. 1990. Energy transfer in the B800–850 antenna complex of purple bacteria *Rhodobacter sphaeroides*: a study by spectral hole-burning. *Chem. Phys. Lett.* 170:231–238.

Vasmel, H., R. J. van Dorssen, G. J. De Vos, and J. Amesz. 1986. Pigment organization and energy transfer in the green photosynthetic bacterium *Chloroflexus aurantiacus*: I. The cytoplasmic membrane. *Photosynth. Res.* 7:281–294.

Wechsler, T. D., R. A. Brunisholz, G. Frank, F. Suter, and H. Zuber. 1987. The complete amino acid sequence of the antenna polypeptide B806–866-β from the cytoplasmic membrane of the green bacterium *Chloroflexus aurantiacus*. *FEBS Lett.* 210:189–194.

Wechsler, T., R. Brunisholz, F. Suter, R. C. Fuller, and H. Zuber. 1985. The complete amino acid sequence of a bacteriochlorophyll *a* binding polypeptide isolated from the cytoplasmic membrane of the green photosynthetic bacterium *Chloroflexus aurantiacus*. *FEBS Lett.* 191:34–38.

Wu, H.-M., S. Savikhin, N. R. S. Reddy, R. Jankowiak, R. J. Cogdell, W. S. Struve, and G. J. Small. 1996. Femtosecond and hole-burning studies of B800's excitation energy relaxation dynamics in the LH2 antenna complex of *Rhodopseudomonas acidophila* (Strain 10050). *J. Phys. Chem.* 100:12022–12033.

Zuber, H., and R. A. Brunisholz. 1991. Structure and function of antenna polypeptides and chlorophyll-protein complexes: principles and variability. *In* Chlorophylls. H. Scheer, editor. CRC Press, Boca Raton. 628–692.